Mimas absorption region (Fig. 4, A and B) occur antisymmetrically at magnetic L coordinates which are larger than expected inbound, in the northern hemisphere, and smaller than expected outbound, in the southern hemisphere. Thus, on the basis of the energetic charged particle data, a simple centered dipole aligned with Saturn's rotation axis is not a satisfactory description of the magnetic field even in the inner magnetosphere. The deviations observed require a modification of the field from the centered, untilted model which is antisymmetric between the northern and southern hemispheres, thus suggesting a north-south offset of the dipole center, or, since our data cover a narrow longitude range, a tilt of the dipole. An equatorial ring current would produce a distortion which is symmetric between the northern and southern hemispheres, and thus cannot account for these observations.

Models of Saturn's magnetic field obtained from analyses of magnetometer data on the Pioneer 11 (*13*) and the Voyager 1 (*14*) spacecraft indicate that the internal field is dipolar. These models have also suggested that the dipole may be slightly tilted relative to Saturn's rotation axis or offset along that axis from the center of the planet. Accordingly, we have reanalyzed our data to determine the tilt and offset which are consistent with the positions of the absorption features that we observed in the inner magnetosphere. In this analysis (based on the predicted spacecraft trajectory) two positions for the dipole were considered: planet-centered and offset 0.04 R_S north. At each of these positions the dipole tilt required to align our observations inbound and outbound was calculated as a function of the longitude direction of the tilt. The results of this analysis (Fig. 7, a and b) indicate that if the dipole were centered on Saturn, the orientation that provides the best description of our data has a tilt of $\sim$ 1° toward longitude (SLS) of 120° to 200°. Alternatively, if the dipole were offset 0.04 R_S north as suggested by Smith *et al.* (*13*), our data are consistent with no tilt ($< 0.5°$), provided that a ring current is included in the model for the Tethys observation (*15, 16*).

These observations are biased, however, since all were obtained over a narrow range of Saturn longitudes (−45° to +8° SLS). Thus these data are less sensitive to any component of the tilt normal to the direction from Saturn to the spacecraft, that is, toward SLS longitudes of 45° to 100° and 225° to 280°. In addition, the nondipolar distortions induced by currents in Saturn's magnetosphere (*15*), which may be expected to have the greatest effect in these data at Tethys, have only crudely been taken into account. With these caveats, our results are inconsistent with the 0.7° to 1.77° dipole tilt toward 324° to 352° SLS deduced from Voyager 1 magnetometer observations (*14*), since for a centered dipole our results suggest a tilt of this magnitude toward the opposite hemisphere.

The most recent, but preliminary, Saturnian magnetic field analysis, obtained by combining Voyager 1 vector and Voyager 2 magnitude data (*3*), yields a centered dipole tilted by 0.8° toward 280° SLS (equivalent to −0.8° toward 100° in Fig. 7, a and b). For this dipole orientation our results suggest a significant northward offset of the dipole (> 0.04 R_S). Clearly, a definitive determination of the structure of Saturn's magnetic field will require a synthesis of these data with the magnetometer observations and must include better estimates of the effects of any current systems operating within Saturn's magnetosphere.

R. E. VOGT
D. L. CHENETTE
A. C. CUMMINGS
T. L. GARRARD
E. C. STONE
California Institute of Technology, Pasadena 91125

A. W. SCHARDT
J. H. TRAINOR
N. LAL
F. B. MCDONALD
NASA Goddard Space Flight Center, Greenbelt, Maryland 20771

References and Notes

1. For a description of the cosmic-ray system on the Voyager 1 and 2 spacecraft, see E. C. Stone, R. E. Vogt, F. B. McDonald, B. J. Teegarden, J. H. Trainor, J. R. Jokipii, W. R. Webber, *Space Sci. Rev.* **21**, 355 (1977).
2. H. S. Bridge *et al.*, *Science* **215**, 563 (1982).
3. N. F. Ness, M. H. Acuña, K. W. Behannon, L. F. Burlaga, J. E. P. Connerney, R. P. Lepping, F. M. Neubauer, *ibid.*, p. 558.
4. R. E. Vogt, D. L. Chenette, A. C. Cummings, T. L. Garrard, E. C. Stone, A. W. Schardt, J. H. Trainor, N. Lal, F. B. McDonald, *ibid.* **212**, 231 (1981).
5. N. F. Ness, personal communication.
6. We define L as $R/\cos^2(\lambda)$, where R is the radial distance from Saturn in Saturn radii (the radius of Saturn is taken to be 60,330 km), and λ is the magnetic latitude.
7. F. B. McDonald, A. W. Schardt, J. H. Trainor, *J. Geophys. Res.* **85**, 5813 (1980).
8. W. Fillius and C. McIlwain, *ibid.*, p. 5803.
9. J. A. Simpson, T. S. Bastian, D. L. Chenette, R. B. McKibben, K. R. Pyle, *ibid.*, p. 5731.
10. J. A. Van Allen, B. A. Randall, M. F. Thomsen, *ibid.*, p. 5679.
11. J. A. Van Allen, M. F. Thomsen, B. A. Randall, *ibid.*, p. 5709.
12. The Saturn longitude system, SLS, used in this report is a Saturn-fixed system with longitude increasing to the west [see M. D. Desch and M. L. Kaiser, *Geophys. Res. Lett.* **8**, 253 (1981)].
13. E. J. Smith *et al.*, *J. Geophys. Res.* **85**, 5655 (1980).
14. M. H. Acuña, J. E. P. Connerney, N. F. Ness, *Nature (London)* **292**, 721 (1981).
15. J. E. P. Connerney, M. H. Acuña, N. F. Ness, *ibid.*, p. 724.
16. J. E. P. Connerney, personal communication.
17. Counting rates in this report were obtained from the following detectors of the cosmic-ray instrument: ($\geq$ 0.43-MeV protons) L1, 2.8 cm^2 × 35 μm, 0.2-MeV threshold; (0.14- to 0.4-MeV electrons) A1, 8 cm^2 × 0.15 mm, 0.1-MeV threshold; ($\geq$ 0.35-MeV electrons) B1, high gain, 8 cm^2 × 2 mm, 0.3-MeV threshold; (1- to 2-MeV electrons) B1, low gain, 8 cm^2 × 2 mm, 1.0-MeV threshold; ($>$ 2.5-MeV electrons) B2, low gain, 8 cm^2 × 2 mm, 2.2-MeV threshold; ($>$ 0.6-MeV electrons) D1, 4.5 cm^2 × 3 mm, 0.5-MeV threshold. See (*1*) for more information.
18. We thank the Voyager project members and the enthusiastic staff of our laboratories at Caltech and Goddard Space Flight Center for their splendid support. Special thanks go to W. Althouse, M. Fernandez, R. Kelly, and I. Matus (Caltech), W. Davis, H. Domchick, and D. Stillwell (Goddard), and O. Divers, E. Franzgrote, and R. Parker (Jet Propulsion Laboratory). Supported by NASA under NAS7-100 and NGR 05-002-160.

10 November 1981

Planetary Radio Astronomy Observations from Voyager 2 Near Saturn

Abstract. *Planetary radio astronomy measurements obtained by Voyager 2 near Saturn have added further evidence that Saturnian kilometric radiation is emitted by a strong dayside source at auroral latitudes in the northern hemisphere and by a weaker source at complementary latitudes in the southern hemisphere. These emissions are variable because of Saturn's rotation and, on longer time scales, probably because of influences of the solar wind and Dione. The electrostatic discharge bursts first discovered by Voyager 1 and attributed to emissions from the B ring were again observed with the same broadband spectral properties and an episodic recurrence period of about 10 hours, but their occurrence frequency was only about 30 percent of that detected by Voyager 1. While crossing the ring plane at a distance of 2.88 Saturn radii, the spacecraft detected an intense noise event extending to above 1 megahertz and lasting about 150 seconds. The event is interpreted to be a consequence of the impact, vaporization, and ionization of charged, micrometer-size G ring particles distributed over a vertical thickness of about 1500 kilometers.*

The Voyager 2 planetary radio astronomy (PRA) instrument (*1*) made observations of several radio wave phenomena during the encounter with Saturn on 26 August 1981. We describe here three of the phenomena: Saturn kilometric radia-

0036-8075/82/0129-0582$01.00/0

tion (SKR), Saturn electrostatic discharges (SED), and a remarkable noise event at the time of ring plane crossing. The Voyager 1 PRA instrument discovered SED during the November 1980 Saturn encounter (*2, 3*), and SKR has been observed by both Voyagers since January 1980 (*2, 4–7*).

Saturn kilometric radiation. Intense SKR dominated the radio spectrum at frequencies below 1 MHz as Voyager 2 approached the planet. After the spacecraft crossed the ring plane and moved into the southern hemisphere, the properties of the SKR changed dramatically. Figure 1 shows dynamic spectra of SKR measured between 1.2 kHz and 1.3 MHz for five consecutive rotations of Saturn spanning the 53-hour period near closest approach. Prior to closest approach (Fig. 1, a and f), the SKR filled the frequency range between 60 and 900 kHz and occasionally extended to frequencies as low as 20 kHz and as high as 1100 kHz. Although the SKR exhibited large fluctuations in intensity as a function of time, some activity is always evident in the two preencounter spectrograms. The SKR polarization was almost exclusively right-hand (RH) before closest approach, although left-hand (LH)–polarized narrowband SKR appeared near 40 kHz from about 180° to 360° Saturn longitude (Fig. 1g). This same morphology, including the narrowband emission, was observed by Voyager 1 as it approached Saturn along a similar northern latitude dayside trajectory (*2*).

The narrowband component of SKR resembles the Jovian narrowband kilometric radiation (*8*) in a number of ways. Both are confined to frequencies near or below 100 kHz; both have bandwidths of only a few tens of kilohertz and exhibit polarization-versus-time patterns that appear to be independent of the polarization of the higher frequency bursts. The Jovian narrowband kilometric radiation is thought to originate from a region near the outer periphery of Io's plasma torus (*8*), and the Voyager plasma science team (*9*) now reports a plasma torus at Saturn which may contain plasma densities and density gradients, in parts of the magnetosphere, that are similar to those encountered in the outer part of Io's torus. Thus, given the apparent similarities between the narrowband components of radio emission from Saturn and Jupiter and between certain aspects of their plasma environments, we suspect that the two emission components originate through similar mechanisms from similar magnetospheric regions. This view has also been advanced in connection with lower frequency banded emission observed by the Voyager 1 plasma wave science instrument at Saturn (*10*). Saturn's narrowband emission (Fig. 1) tends to occur at somewhat lower frequencies than Jupiter's, and this is consistent with the observation of relatively lower electron densities in Saturn's plasma torus than in the Io torus.

Nearly 1 hour before closest approach (Fig. 1, c and h), the SKR vanished entirely and did not reappear until about 2 hours after closest approach. During this interval the only detectable activity was associated with SED, with the brief, broadband event recorded during crossing of the ring plane at 0418 spacecraft event time (SCET), and with electrostatic plasma waves at low-order, odd, half-harmonics of the electron gyrofrequency. Thus the SKR source apparently was occulted or beamed away from the spacecraft when Voyager 2 was within about 1 Saturn radius of the planet's equatorial plane (between 2000 and 0100 hours local solar time). This occultation is consistent with a northern hemisphere source region (for the RH-polarized SKR) near the noon meridian at high latitudes (*6*).

When the SKR reappeared at about 0535 SCET on 26 August 1981, its polarization was reversed from that observed during the preencounter interval, and thereafter it remained exclusively LH. This pattern of RH polarization for SKR observed from above northern latitudes and LH polarization for SKR observed from above southern latitudes is exactly what Voyager 1 found (*2*). LH-polarized SKR was detected only during the 23-hour period when Voyager 1 was in the southern hemisphere. As before, we associate LH-polarized emission with a source in the southern hemisphere. With regard to the intensity of the emission, however, the Voyager 2 measurements differ from the Voyager 1 data in that the SKR rapidly drops in intensity and bandwidth soon after its postencounter reappearance. For example, notice, in the lower two sets of dynamic spectra in Fig. 1, that on the first full Saturn rotation after closest approach the low-frequency limit of SKR has drifted up to ~ 200

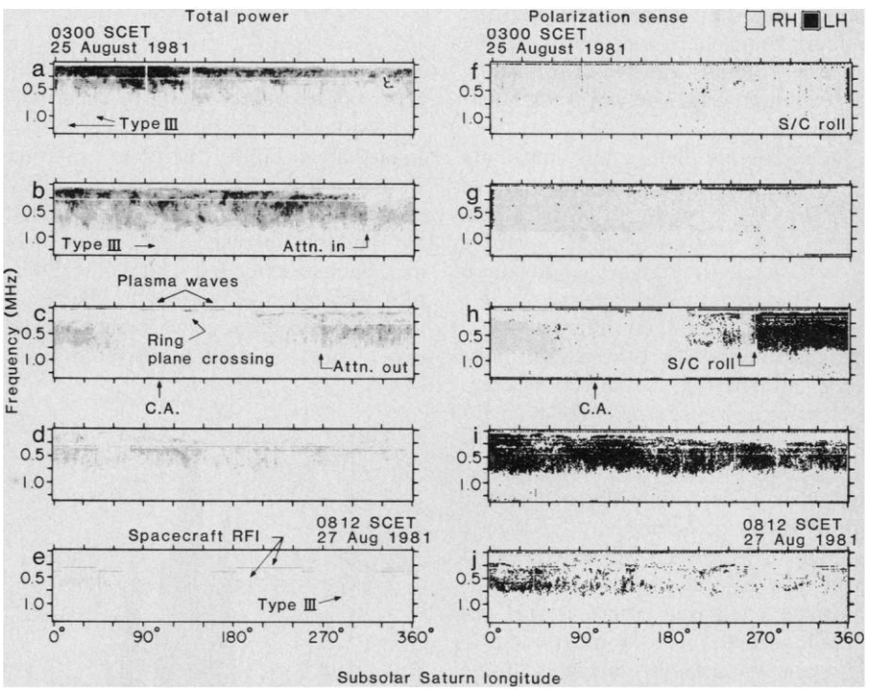

Fig. 1. Dynamic spectra of SKR emissions observed during the five consecutive 10.66-hour rotations of Saturn centered on the time of Voyager 2 closest approach (*C.A.*). The panels are aligned with respect to subsolar Saturn longitude, and each panel is formed from averages over 1° increments of longitude (1.8 minutes) at each of 70 frequency channels spaced at 19.2-kHz intervals between 1.2 and 1326 kHz. (a to e) Total intensity, encoded so that increasing darkness denotes increasing intensity; (f to j) dominant sense of circular polarization, encoded so that gray denotes RH polarization and black denotes LH polarization. Near the time of closest approach and ring plane crossing (c and h), the SKR disappeared and only very low frequency in situ plasma waves and the ring plane burst were detected. There were brief reversals in polarization during spacecraft rolls, when Saturn moved to the opposite hemisphere relative to the plane of the PRA antennas, and a major RH to LH reversal occurred after closest approach, when Voyager 2 moved from northern to southern latitudes. The plots also show the effects observed when a 15-dB attenuator was inserted in the receiver preamplifier and when several non-Saturnian signals occurred (solar type III bursts and spacecraft radio frequency interference).

kHz. By the end of the last rotation in Fig. 1 the few bursts that can be detected are seen only at frequencies between about 500 and 800 kHz. Based on qualitative examination of the LH emission observed by both Voyagers, we conclude that the southern hemisphere source, like the northern hemisphere source, is on the dayside and at high latitudes.

The change in Saturn's kilometer wavelength spectrum is illustrated quantitatively in Fig. 2, which displays the normalized median power flux density for the two Saturn rotations before and after closest approach. The maximum flux density inbound occurred near 175 kHz, similar to the Voyager 1 observation (*6*). The maximum flux density outbound occurred near 500 kHz and was approximately three orders of magnitude weaker than the inbound emission. Figure 2 also shows the outbound spectrum observed by Voyager 1 (*6*) from the conjugate latitude in the northern hemisphere relative to the Voyager 2 outbound observation (3.5 hours solar local time, 26°N for Voyager 1; ~ 4.0 hours local time, 27°S for Voyager 2). Here we also see that the LH emission from the southern hemisphere was approximately two orders of magnitude weaker than the RH emission from the northern hemisphere.

Three different factors may contribute to the apparent north-south difference in SKR activity. First, the southern hemisphere SKR may be beamed toward a different local time than the northern SKR. This would mean that spectra like those in Fig. 2 are from different points on the northern and southern SKR emission beam patterns, making direct comparisons impossible. One of the goals for the Voyager 2 encounter, especially during the outbound portion of the trajectory, was to determine the occurrence rate of southern hemisphere SKR as a function of longitude. Since Voyager 1 spent only a brief period south of the Saturnian equatorial plane, it was not possible to determine the longitude profile unambiguously. From Fig. 1, d and e, and from more recent data, it appears that the southern hemisphere SKR is greatest approximately 100° east of the northern hemisphere emission. However, although the data appear to be consistent with a dayside source, it is not possible to deduce the exact local time of the source region until data representing a longer time span are analyzed.

The second possible explanation for the observed north-south radio intensity difference is that the SKR diminished just after closest approach as a consequence of temporal variations in the energy source. In fact, there is some indirect evidence to support this hypothesis. Immediately after the last rotation shown in Fig. 1, SKR was essentially undetectable for 2 to 3 days, after which the emission returned and seemed normal. Such an extended period of inactivity is very unusual and may be the result of solar wind pressure variations. However, since a similar north-south radio asymmetry was noted during the Voyager 1 encounter (*2*), it seems unlikely that all the differences can be attributed solely to coincidental, external causes.

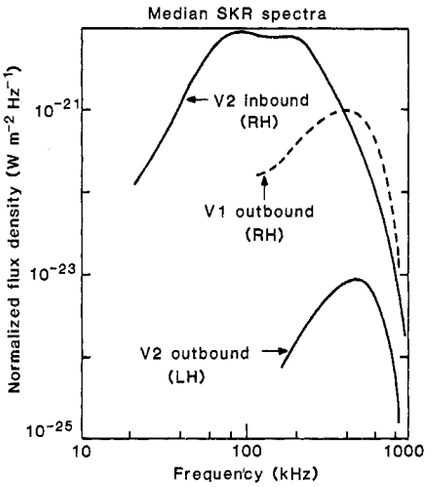

Fig. 2. Spectra formed from the median values of power flux density observed over the period before closest approach of Voyager 2 (Fig. 1, a and b) and the period after closest approach (Fig. 1, d and e) and over the month after closest approach of Voyager 1. The Voyager 2 inbound and Voyager 1 outbound data are dominated by the RH-polarized emissions observed from northern latitudes, and the Voyager 2 outbound spectrum is dominated by the LH-polarized emissions observed from southern latitudes. All flux densities are normalized to an equivalent observer to Saturn distance of 1 AU.

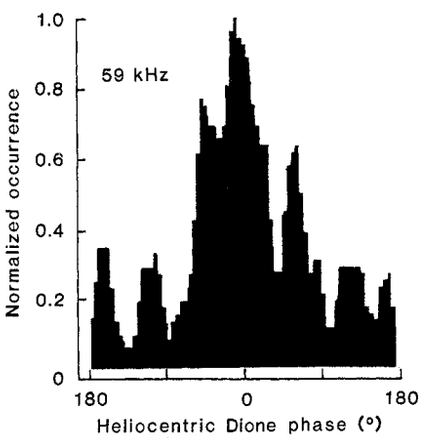

Fig. 3. Histogram showing the relation between SKR and heliocentric Dione phase from 1 through 24 August. The histogram is comprised of events recorded at 59 kHz and includes only events with flux density exceeding 2×10^{-21} W/m^2-Hz for an observer situated 1 AU from Saturn (to eliminate inverse-distance-squared bias).

Finally, there may be an intrinsic difference between the northern and southern radio sources. Intrinsic north-south differences may be associated with differences between the external current systems or between particle entry into the northern and southern SKR source regions. Or, if the radio emission originates in the dayside cusp regions, a long-term periodic difference between northern and southern radio emission properties might exist due to the geometry of Saturn and the sun. During the Voyager observations, the flux of solar wind particles into the northern cusp might have exceeded the flux into the southern cusp because the northern cusp was tilted toward the sun, by 4° during the Voyager 1 flyby and by 7° during the Voyager 2 flyby. We conclude that the southern source is intrinsically weaker than the northern source, that both sources are located in the sunward hemisphere, and that there were substantial temporal variations (exceeding 1 day) in the activity of the sources shortly after closest approach of Voyager 2.

For several months before and for several days after the encounter of Voyager 2 with Saturn, the SKR exhibited temporal variations of a kind never seen before. These fluctuations took the form of well-defined, dramatic decreases in emission activity lasting from about four to eight Saturn rotations, depending on the interval examined. In each fluctuation we have studied, the emission intensity dropped below receiver threshold over the entire SKR bandwith (~ 1 MHz) for the duration of the dropout. An example of the beginning of such an event is shown in Fig. 1e. Here it is apparent that the SKR has begun to diminish in intensity far faster than that due to inverse-distance-squared falloff. The SKR continued to diminish, and was below receiver threshold at all frequencies for about 2 days until reappearing at about 0800 SCET on 29 August. Normalized to an observer to Saturn distance of 1 AU, this threshold represents an emission flux upper limit for the southern hemisphere source of about 10^{-24} W/m^2-Hz (see Fig. 2 for nominal flux levels).

We have identified six similar dropout intervals in the July to August Voyager 2 data. These occurred earlier than the one described here. Since the northern and, to some extent, southern hemisphere sources were observed before encounter and since neither source appeared during a cutoff interval, both sources must have

been affected by the same mechanism. In addition, we have found no comparable dropout periods in the data obtained by Voyager 1 during the 3-month period surrounding its encounter in November 1980. Thus, because this phenomenon appears unique to the Voyager 2 encounter and because the 26 to 27 August episode occurred when Saturn's magnetosphere apparently was inflated (*11*) due to extremely low solar wind flux, we are examining the possibility that the episodes are related to occasions when Saturn is immersed in Jupiter's magnetic tail (*12*). This interpretation is particularly appealing because, if the SKR emanates from the vicinity of the dayside polar cusps (*6*), a strong reduction in solar wind pressure might be expected to diminish the particle population in the cusp region and yield the observed result. If this interpretation is correct, then the time scale of the radio emission turnoff would appear to be approximately 2 days, since Ness *et al.* (*11*) identify the onset of the ram pressure decrease at about 1000 hours SCET on 25 August 1981.

If Jupiter's tail or large-scale changes in solar wind pressure prove effective in extinguishing SKR, it would be the second modulator of Saturn's radio emission. Dione was first suggested (*7, 13*) as the cause of the disappearance of SKR at times when the radiation normally would be observed. We have tried to separate these two effects by taking advantage of the strong frequency dependence of the Dione modulation (*7*) compared with the very broadband quenching characteristic of the 2- to 3-day dropouts. Thus, we were able to examine the preencounter period 1 to 24 August for evidence of any Dione-induced modulation by eliminating the interval 9 to 10 August, which clearly was a broadband, long-term dropout. The result is shown in Fig. 3. Here activity at 59 kHz is organized at Dione's period of revolution (65.7 hours), and heliocentric orbital phase runs from 180° through 360° to 180° (for clarity). The histogram is evidence for a strong modulation of SKR by Dione, and it represents yet another way in which modulation appears at Dione's period. Previous reports showed quenching of SKR near 270° (*7, 13*) and 40° Dione phase (*7*). The present analysis, however, reveals not only a shift in the phase of effective quenching to around 180° but also what might be interpreted as a stimulation of activity levels rather than a quenching; the peak in Fig. 3 is sharper than the absorption minimum by at least a factor of 2. The nature of Dione's modulating effect may become clearer on examination of the data obtained when Voyager 2 was outbound, that is, when the aspect angle of the observations was very different.

Saturn electrostatic discharges. A new phenomenon, SED, was discovered by the Voyager 1 PRA instrument (*2, 3*). An example of SED on dynamic spectrograms is shown in Fig. 4. SED were also observed during the Voyager 2 encounter with Saturn, and many features appear to be the same as before. However, there are some striking differences.

The SED were again impulsive, lasting for 30 msec or less to 250 msec, and again appeared to be randomly distributed over a frequency range extending from 100 kHz or less to at least 40 MHz, the highest frequency attainable by the PRA instrument. As before, the SED occurred in episodes lasting several hours (Fig. 5) and were detected only during the 6 or 7 days surrounding closest approach. This fact, together with the similarities in event duration and frequency distribution, suggests that the intensity of SED did not change significantly between encounters. Voyager 2 detected SED more than 48 hours before the first inbound bow shock crossing, so they clearly are not due to phenomena occurring at the spacecraft inside Saturn's magnetosphere.

The rate of occurrence of SED im-

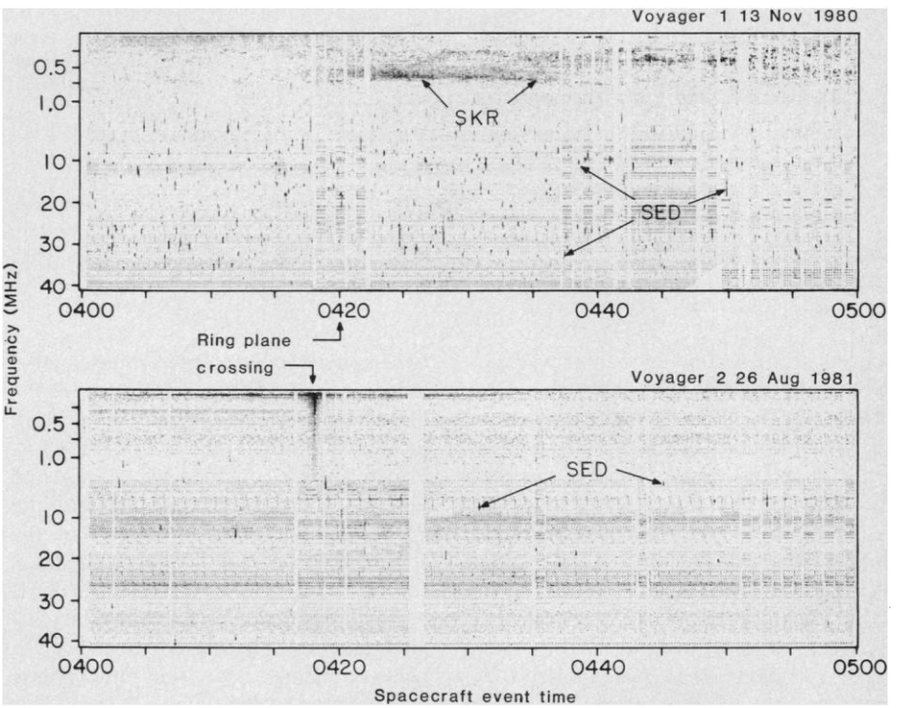

Fig. 4. Dynamic spectra of observations obtained between 1.2 kHz and 40.5 MHz with 6-second temporal resolution over 1-hour intervals spanning the outbound ring plane crossing by Voyager 1 at a distance of 6.3 R_S (upper panel) and the ring plane crossing by Voyager 2 at 2.9 R_S (lower panel). SED appear as bursts lasting less than 1 second and occur at whatever frequency the receiver was tuned to at that instant. Notice that the SKR is evident below 1 MHz for the Voyager 1 ring plane crossing segment but not for the Voyager 2 segment, that the brief ring plane crossing burst extends to above 1 MHz for Voyager 2 but is not conspicuous for Voyager 1, and that the SED bursts are much less frequent for Voyager 2 than for Voyager 1.

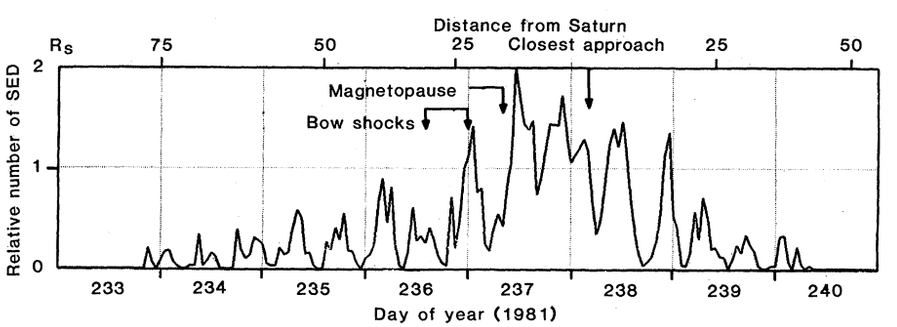

Fig. 5. Saturn electrostatic discharges organized into distinct episodes separated by about 10 hours. Note that the SED were observed several days before Voyager 2 entered the Saturnian magnetosphere. The greatest number of SED occur near closest approach.

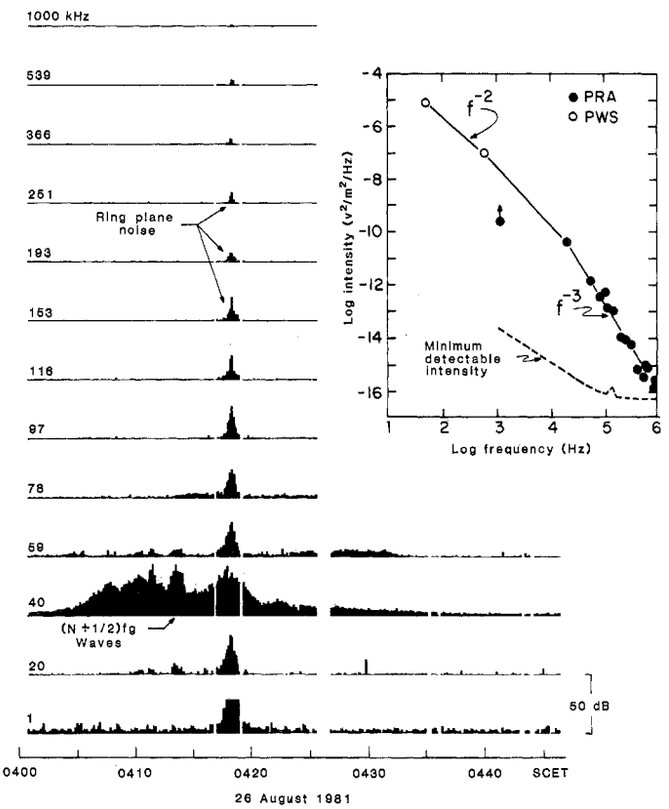

Fig. 6. Relative intensity measured at 13 selected frequency channels between 1.2 and 1000 kHz during the Voyager 2 ring plane crossing. The inset shows the field intensity spectrum measured at the peak of the ring plane event (0418 SCET) by the PRA instrument and by two channels of the plasma wave science instrument (*14*).

pulses at the second encounter was only about one-third of that at the first (Fig. 4). In addition, the episodes themselves were distributed much more symmetrically about the time of closest approach (most of the Voyager 1 episodes occurred after the Voyager 1 encounter).

Before and during closest approach of Voyager 1, fewer than 1 percent of the SED events were polarized, whereas afterward 90 to 95 percent of the events above 15 MHz were LH-polarized (*3*). Furthermore, the proportion of polarized events diminished with decreasing frequency. During the Voyager 2 encounter, however, most of the polarization occurred in channels below 5 MHz. Approximately 5 to 10 percent of the events in these channels displayed polarization, with roughly as many RH as LH. This pattern persisted throughout the encounter. Thus, although Voyager 2 confirmed the SED phenomenon, the striking differences in polarization, episode distribution, and number of events strongly suggest a source that changes with time.

Analysis of the Voyager 2 data yields a repetition period for SED episodes of about 10 hours. This is consistent with the period determined from the Voyager 1 data (10 hours 10 ± 5 minutes) (*3*), and clearly different from Saturn's period of rotation (10 hours 39.4 ± 0.1 minutes) (*5*). The phase of the repetition period is fixed relative to the line between planet and observer, implying that the source of SED rotates (or revolves) like a searchlight and is not fixed relative to the sun, as is the case for SKR. Previously we concluded (*2*, *3*) that the repetition rate of SED episodes and the "searchlight" behavior imply that the source of SED is not similar to the SKR source. Also, the observation of SED bursts at frequencies well below the plasma frequency of Saturn's ionosphere virtually eliminates any sort of atmospheric phenomenon as the cause of SED. This information, combined with the 10-hour 10-minute repetition period, led us to conclude (*2*, *3*) that the source of SED was in the ring system about 1.81 Saturn radii (R_S) from the center of the planet. The Voyager 2 observations reported here in no way change our original thesis.

Ring plane event. The PRA instrument on Voyager 2 also detected an intense event at or near the time of ring plane crossing (Figs. 4 and 6). Power in the PRA channels peaked at 0418:17 SCET on day 238 (26 August 1981). The distance of the spacecraft from Saturn at ring plane crossing was approximately 2.88 R_S, near the nominal 2.82 R_S location of the G ring.

The time profile of the PRA event was generally symmetrical about the peak. The central peak displays a half-power rise time of 6 seconds or less, and the overall pattern exhibits a 30-dB rise time of approximately 1 minute. These times correspond to distances of about 70 and 700 km, respectively, normal to the ring plane. At its peak, the ring plane event extended from frequencies of 10 Hz or less to approximately 1 MHz, and the spectrum peaked in the 56-Hz channel of the plasma wave science instrument (*14*). The spectral density over five decades in frequency is shown in the inset to Fig. 6. The emission showed no evidence of polarization in any of the PRA channels. A similar event may have occurred when Voyager 1 crossed the ring plane outbound (*15*); however, the essential features of that event are difficult to extract because of strong plasma wave phenomena and SKR emissions.

The ring plane event is distinct from both SKR and SED in onset, duration, spectral character, and polarization (*2*–*4*); the associated mechanism, we presume, is also distinct. The plasma instrument on Voyager 2 measured a nominal plasma concentration of approximately 100 particles per cubic centimeter during the ring plane crossing (*9*). Thus the ambient plasma frequency was at least 100 kHz, which is well above the frequency at which the event spectrum peaked. Therefore the observed emissions evidently are not propagating electromagnetic disturbances originating at Saturn or in any of its rings, including the G ring. On the contrary, the phenomenon appears to originate at the spacecraft.

Warwick *et al.* (*2*) suggested that charged dielectric particles striking the PRA antenna booms could generate electrical events. Micrometer-size ice particles striking the spacecraft at relative velocities of 10 km/sec or more probably would vaporize and ionize. In the G ring most particles are believed to be 1 to 5 μm in diameter (*16*), and Clark (*17*) deduced that the composition of Saturn ring material is approximately 95 percent water ice and 5 percent ferric oxide. The spacecraft velocity relative to G ring material was about 14 km/sec at the time of ring plane crossing.

We propose the following simple model of the ring plane event. At or near the time of ring plane crossing, Voyager 2 strikes charged micrometer-size ice particles in the outer regions of the G ring. The 56-Hz spectral peak is taken to be an approximate measure of the impact frequency. Each impact produces a tenuous charged plasma enveloping part or all of the spacecraft. The plasma dissipates because of thermal motion and relative motion between the spacecraft and Saturn's corotating magnetic field, in which

the plasma becomes embedded. A typical dissipation time is 0.5 msec. Since this is short compared to the inferred impact frequency, the phenomenon is dominated by single events. The step-function increases in voltage associated with the production of charged plasma exhibit an f^{-2} flux density spectrum; however, such a spectrum is modified at low frequencies by the impact rate itself and at high frequencies by dissipation effects and plasma physical phenomena. Additional modifications could result from spacecraft interactions with the plasma. Therefore, an impact discharge phenomenon could produce a spectrum like that shown in Fig. 6.

In this model, the Voyager 2 PRA and plasma wave science instruments act in tandem to yield in situ measurements of G ring material. The falloff in intensity and the change in spectrum away from the ring plane are attributed to variations in particle size and number density along the path of the spacecraft. The total vertical thickness of ~ 1500 km inferred from the duration of the ring plane noise event is much greater than the optical thickness reported for any of Saturn's major rings. Hence, these data indicate that the G ring possesses a tenuous halo that extends well beyond the nominal ring particle layer—much like the E ring with its 1800-km inferred thickness (*18*).

J. W. WARWICK
D. R. EVANS, J. H. ROMIG
Radiophysics, Inc.,
Boulder, Colorado 80301
J. K. ALEXANDER
M. D. DESCH, M. L. KAISER
Laboratory for Extraterrestrial Physics,
Goddard Space Flight Center,
Greenbelt, Maryland 20771
M. AUBIER, Y. LEBLANC
A. LECACHEUX, B. M. PEDERSEN
Observatoire de Paris,
Section d'Astrophysique de Meudon,
92190 Meudon, France

References and Notes

1. The PRA instrument has a pair of orthogonal, 10-m, monopole antennas and a 198-channel step-frequency receiver to measure the intensity and circular polarization of radio signals between 1.2 kHz and 40.5 MHz [see J. W. Warwick *et al.*, *Space Sci. Rev.* **21**, 309 (1977)].
2. J. W. Warwick *et al.*, *Science* **212**, 239 (1981).
3. D. R. Evans, J. W. Warwick, J. B. Pearce, T. D. Carr, J. J. Schauble, *Nature (London)* **292**, 716 (1981).
4. M. L. Kaiser, M. D. Desch, J. W. Warwick, J. B. Pearce, *Science* **209**, 1238 (1980).
5. M. D. Desch and M. L. Kaiser, *Geophys. Res. Lett.* **8**, 253 (1981).
6. M. L. Kaiser, M. D. Desch, A. Lecacheux, *Nature (London)* **292**, 731 (1981).
7. M. D. Desch and M. L. Kaiser, *ibid.*, p. 739.
8. M. L. Kaiser and M. D. Desch, *Geophys. Res. Lett.* **7**, 389 (1980).
9. H. S. Bridge *et al.*, *Science* **215**, 563 (1982).
10. D. A. Gurnett, W. S. Kurth, F. L. Scarf, *Nature (London)* **292**, 733 (1981).
11. N. F. Ness *et al.*, *Science* **215**, 558 (1982).
12. F. L. Scarf *et al.*, *Nature (London)* **292**, 585 (1981).
13. W. S. Kurth, D. A. Gurnett, F. L. Scarf, *ibid.*, p. 742.
14. F. L. Scarf *et al.*, *Science* **215**, 587 (1982).
15. B. M. Pedersen *et al.*, *Nature (London)* **292**, 714 (1981).
16. R. J. Terrile, private communication.
17. R. N. Clark, *Icarus* **44**, 388 (1980).
18. D. H. Humes, R. L. O'Neal, W. H. Kinard, J. M. Alvarez, *Science* **207**, 443 (1980).
19. We thank R. Holtzman and his staff at the Jet Propulsion Laboratory for computer support during the encounter period and R. Elson and B. Razzaghinejad for computer support throughout the mission. We also thank the other members of the PRA team, especially R. L. Poynter, for their support. The PWS, PLS, and MAG teams provided invaluable information. Our French investigators acknowledge support by Centre National d'Etudes Spatiales. Supported in part by NASA contract NAS 7-100.

10 November 1981

Voyager 2 Plasma Wave Observations at Saturn

Abstract. *The first inbound Voyager 2 crossing of Saturn's bow shock [at 31.7 Saturn radii (R_S), near local noon] and the last outbound crossing (at 87.4 R_S, near local dawn) had similar plasma wave signatures. However, many other aspects of the plasma wave measurements differed considerably during the inbound and outbound passes, suggesting the presence of effects associated with significant north-south or noon-dawn asymmetries, or temporal variations. Within Saturn's magnetosphere, the plasma wave instrument detected electron plasma oscillations, upper hybrid resonance emissions, half-gyrofrequency harmonics, hiss and chorus, narrowband electromagnetic emissions and broadband Saturn radio noise, and noise bursts with characteristics of static. At the ring plane crossing, the plasma wave instrument also detected a large number of intense impulses that we interpret in terms of ring particle impacts on Voyager 2.*

The Voyager 1 and Voyager 2 trajectories through Saturn's magnetosphere were designed to differ in their distances of closest approach and ring plane crossing and directions of arrival and departure; information from Voyager 2 was expected to supplement and extend the earlier measurements by Voyager 1 (*1*) of plasma wave phenomena and wave-particle interactions. We have found that many of the August 1981 Voyager 2 wave observations, such as the measurements of electromagnetic hiss, chorus, narrowband emissions, and certain impulses in Saturn's inner magnetosphere, can be related to corresponding measurements obtained during the November 1980 Voyager 1 encounter. Other aspects of the Voyager 2 wave observations differed, however, especially during the outbound passage; these differences suggest the presence of effects associated with significant north-south or noon-dawn asymmetries, temporal variations associated with fluctuating solar wind conditions, or proximity to the Jupiter tail and wake (*2*). Another significant difference on Voyager 2 occurred at the close-in ring plane crossing ($R \approx 2.88\ R_S$), where the plasma wave instrument detected a large number of intense impulses that we interpret in terms of ring particle impacts on Voyager 2.

Magnetospheric size. One striking indication that Saturn's magnetosphere had changed by the time of the Voyager 2 encounter comes from comparison of the positions of the first and last crossings of the bow shock, which are marked in Fig. 1C. The dashed curves show the Voyager 1 trajectory and the nominal Voyager 1 bow shock surface in cylindrical coordinates, X versus $(Y^2 + Z^2)^{1/2}$; the heavy solid curve gives the corresponding Voyager 2 encounter trajectory. Figure 1, A and B, displays the plasma wave measurements for the first Voyager 2 inbound shock crossing [1337 spacecraft event time (SCET) on 24 August 1981, at 31.7 R_S, near local noon] and the last outbound crossing (0109 on 31 August 1981, at 87.4 R_S, near local dawn). It is noteworthy that these wave measurements are so similar, although the location of the final outbound crossing was about twice as far from Saturn as would be expected from scaling of the Voyager 1 shock surface out to intersect the Voyager 2 inbound crossing point.

The Voyager 2 plasma probe detected highly variable solar wind pressure before 24 August (*3*), and our measurements of intense upstream plasma oscillations at $f \approx 1.8$ kHz just before 1337 indicate that the local solar wind density (N) was near 0.04 particle per cubic centimeter just before this shock crossing. Since 3.1-kHz electron plasma oscillations (corresponding to $N \approx 0.11\ \text{cm}^{-3}$) were detected in a similar upstream location on Voyager 1 (*4*), the lower wind pressure at the Voyager 2 encounter seems to explain the somewhat bigger magnetosphere detected near local noon (with first shock crossing at 32 R_S rather than at 26 R_S). However, these simple density considerations do not seem able to account for the great distance to the

0036-8075/82/0129-0587$01.00/0